Sandra Steiner
Christine L. Gatlin
John J. Lennon
Andrew M. McGrath
Angel M. Aponte
Anthony J. Makusky
Maria C. Rohrs
N. Leigh Anderson

[1]Large Scale Proteomics Corporation, Rockville, MD, USA

Proteomics to display lovastatin-induced protein and pathway regulation in rat liver

Lovastatin is a lipid lowering agent that acts by inhibiting 3-hydroxy-3-methylglutaryl-coenzyme A (HMG-CoA) reductase, a key regulatory enzyme in cholesterol biosynthesis. In this study the pattern of gene network regulation induced in hepatic proteins as a response to lovastatin treatment was analyzed by proteomics. In livers of male F344 rats treated with 1.6 mg/kg/day lovastatin or 150 mg/kg/day lovastatin for seven days, 36 proteins were found to be significantly altered ($p<0.001$) in relation to treatment. The changed proteins were classified according to their cellular function and participation in biochemical pathways. The following observations were made: (i) inhibition of HMG-CoA reductase provoked a regulatory response in the cholesterol synthesis pathway including the induction of cytosolic HMG-CoA synthase and of isopentenyl-diphosphate delta-isomerase, (ii) manipulation of the lipid metabolism triggered alterations in key enzymes of the carbohydrate metabolism, and (iii) lovastatin treatment was associated with signs of toxicity as reflected by changes in a heterogeneous set of cellular stress proteins involved in functions such as cytoskeletal structure, calcium homeostasis, protease inhibition, cell signaling or apoptosis. These results present new insights into liver gene network regulations induced by lovastatin and illustrate a yet unexplored application of proteomics to discover new targets by analysis of existing drugs and the pathways that they regulate.

Keywords: Lovastatin / Proteomics / Rat liver / Two-dimensional electrophoresis / Mass spectrometry / Pathway regulation EL 3978

1 Introduction

Epidemiological studies have established that both high levels of low density lipoprotein (LDL) cholesterol as well as low levels of high density lipoprotein (HDL) cholesterol are risk factors for coronary heart disease. In addition, the involvement of LDL cholesterol in atherogenesis has been well documented in clinical studies. Cholesterol is synthesized predominantly in the liver and transported to various body tissues by lipoproteins in blood plasma. Therapeutic interventions to normalize elevated plasma LDL cholesterol levels in hypercholesterolemic individuals are in widespread use. Of these, 3-hydroxy-3-methylglutaryl-coenzyme A (HMG-CoA) reductase inhibitors have become the most widely prescribed family of agents (lovastatin, pravastatin, simvastatin, fluvastatin, atorvastatin). HMG-CoA reductase is the key regulatory enzyme in the biosynthetic pathway for cholesterol and catalyzes the conversion of HMG-CoA to mevalonate. The inhibition of this enzyme results in both the downregulation of cholesterol synthesis and the upregulation of hepatic high affinity receptors for LDL followed by increased catabolism of LDL cholesterol [1]. Otherwise, HMG-CoA reductase inhibitors do not affect the levels and/or composition of the other major lipoprotein fractions [2] to a significant extent.

The HMG-CoA reductase inhibitor lovastatin is a molecule derived from a strain of the fungus *Aspergillus terreus* and is sold under the brand name Mevacor® in the United States. It is administered as a prodrug in its lactone form and undergoes first-pass metabolism, hepatic sequestration and hydrolysis to the active form [3]. Thus, lovastatin appears in much higher concentrations in the liver than in nontarget organs, and the liver is the drug's primary site of both action and side effects. Marked increases in serum transaminases and biochemical abnormalities of liver function occurred in a subset of patients who received lovastatin or other HMG-CoA reductase inhibitors for an extended period of time [4].

It is straightforward to imagine that the therapeutic inhibition of a key enzyme of the cholesterol synthesis pathway is not silently tolerated by the organism but evokes a response targeted to compensate for disturbed pathway

Correspondence: Dr. Sandra Steiner, Large Scale Proteomics Corporation, 9620 Medical Center Drive, Suite 201, Rockville, MD 20850, USA
E-mail: sandra.steiner@lsbc.com
Fax: +301-762-4892

Abbreviations: HDL, high density lipoprotein; **HMG-CoA**, 3-hydroxy-3-methylglutaryl-coenzyme A; **IPP-isomerase**, isopentenyl-diphosphate delta-isomerase; **LDL**, low density lipoprotein; **NR**, nonredundant

 0173-0835/00/1111-2129 $17.50+.50/0

performance. Such a regulatory feedback effect may contribute to the pharmacological action of a drug, *e.g.*, the upregulation of LDL receptors [5], but equally is often associated with adverse reactions. The purpose of this study was to gain molecular insights into the liver effects induced by lovastatin and to elucidate the biochemical pathways and gene network regulations induced downstream of the blockade of HMG-CoA reductase. Tissue proteome analysis has been successfully applied [6–12] to investigate the molecular effects of drugs and to obtain information on their mode of action and mechanisms of toxicity. In this case, we used proteomics to study proteome changes in livers of rats treated for seven days with either 1.6 or 150 mg/kg/day lovastatin. The drug was found to induce a complex pattern of alterations in rat liver proteins, some of which were related to cholesterol synthesis but many were representing effects on other pathways and endpoints.

2 Material and methods

2.1 Reagents

Ultrapure reagents for polyacrylamide gel preparation were obtained from Bio-Rad (Richmond, CA). Carrier ampholytes pH 4–8 were from BDH (Poole, UK), carrier ampholytes, pH 8–10.5, were from Pharmacia (Uppsala, Sweden) and CHAPS was obtained from Calbiochem (La Jolla, CA). Deionized water from a high-purity water system (Neu-Ion, Baltimore, MD) was used. System filters are changed monthly to ensure 18MΩ purity. HPLC grade methanol and glacial acetic acid were furnished from Fisher Scientific (Fair Lawn, NJ). HPLC grade acetonitrile was obtained from Baker (Phillipsburg, NJ). Dithiothreitol (DTT) was obtained from Gallard-Schlesinger Industries (Carle Place, NY). Iodoacetamide, ammonium bicarbonate, trifluoroacetic acid and α-cyano-4-hydroxycinnamic acid were obtained from Sigma Chemical (St. Louis, MO). Modified porcine trypsin was purchased from Promega (Madison, WI). All chemicals (unless specified) were reagent grade and used without further purification.

2.2 Animal treatment protocol

Male F344 rats (Charles River, Raleigh, NC), 8 weeks of age and weighing 167–182 g, were used. The animals were housed individually in rat gang cages in an environmentally controlled room and were fed with Rodent Chow (Research Diets, New Brunswick, NJ) and tap water *ad libitum*. Three groups of five rats each received control feed, rodent chow milled with 16 ppm (approximately 1.6 mg/kg/day) lovastatin and rodent chow milled with 1500 ppm (approximately 150 mg/kg/day) lovastatin for 7 days. The animals were guillotined after CO_2 asphyxiation one day following the last treatment. Liver samples (150 mg of the left apical lobe) were removed and flash-frozen in liquid nitrogen and kept at –80°C until analysis.

2.3 Sample preparation

The samples were homogenized in eight volumes of 9 M urea, 2% CHAPS, 0.5% dithiothreitol (DTT) and 2% carrier ampholytes, pH 8–10.5. The homogenates were centrifuged at 420 000 × *g* at 22°C for 30 min (TL100 ultracentrifuge, TLA 100.3 rotor, 100 000 rpm; Beckman Instruments, Palo Alto, CA). The supernatant was removed, divided into four aliquots and stored at –80°C until analysis.

2.4 Two-dimensional gel electrophoresis

Sample proteins were resolved using the 20 × 25 cm ISO-DALT 2-D system [13]. Eight μL of solubilized sample were applied to each gel, and the gels were run for 25 050 Vh using a progressively increasing voltage with a high-voltage programmable power supply. An Angelique™ computer-controlled gradient-casting system (Large Scale Proteomics, Rockville, MD) was used to prepare the second-dimensional SDS slab gels. The top 5% of each gel was 11%T acrylamide and the lower 95% of the gel varied linearly from 11 to 19%T. The IEF gels were loaded directly onto the slab gels using an equilibration buffer with a blue tracking dye and were held in place with a 1% agarose overlay. Second-dimensional slab gels were run overnight at 160 V in cooled DALT tanks (10°C) with buffer circulation and were taken out when the tracking dye reached the bottom of the gel. Following SDS electrophoresis, the slab gels were fixed overnight in 1.5 L/10 gels of 50% ethanol / 3% phosphoric acid and then washed three times for 30 min in 1.5 L/10 gels of cold deionized water. They were transferred to 1.5 L/10 gels of 34% methanol / 17% ammonium sulfate / 3% phosphoric acid for 1 h, and after the addition of 1 g powdered Coomassie Blue G-250 the gels were stained for three days to achieve equilibrium intensity.

2.5 Quantitative gel pattern analysis

Stained slab gels were digitized in red light at 133 μm resolution, using an Eikonix 1412 scanner (Ektron, Bedford, MA) and images were processed using the Kepler software system as described [13]. Groupwise statistical comparisons were made to search for treatment-related protein abundance changes.

2.6 Protein digestion

Gel pieces containing the proteins of interest were manually excised from a Coomassie stained gel and placed in a 96-well polypropylene microtiter plate. Samples were

in-gel digested with trypsin according to the procedure of Shevchenko *et al.* [14] with slight modifications. Briefly, the excised samples were destained by two 60 min cycles of bath sonication in 0.2 M NH_4HCO_3 in 50% CH_3CN with the resulting solution aspirated after each cycle. A volume of 0.2 M NH_4HCO_3 in 50% CH_3CN to sufficiently cover the gel pieces was added. Reduction and alkylation was accomplished by adding 135 nmol DTT and incubating at 37°C for 20 min. After cooling, 400 nmol of iodoacetamide was added and incubated at room temperature in the dark for 20 min. The supernatant was removed and the samples were washed for 15 min in 0.2 M NH_4HCO_3 in 50% CH_3CN. The gel pieces were dried at 37°C for 15 min and partially rehydrated with 5 μL 0.2 M NH_4HCO_3. After dispensing 3 μL of trypsin (30 ng/μL), the samples were incubated at room temperature for 5 min. A sufficient volume of 0.2 M NH_4HCO_3 was added to ensure complete submersion of the gel pieces in the digestion buffer. Samples were incubated overnight at 37°C. All samples were acidified with 1 μL glacial acetic acid. Tryptic peptides were extracted by initially transferring the digest supernatant to a clean 96-well polypropylene microtiter plate with two subsequent extraction and transfer cycles of 60 μL of 60% CH_3CN, 1% glacial acetic acid. The combined extraction supernatant was dried and reconstituted in 6 μL 1% glacial acetic acid for subsequent mass spectral analysis.

2.7 MALDI-MS for protein identification

All samples were prepared using α-cyano-4-hydroxycinnamic acid as the MALDI matrix utilizing the dried droplet method [15]. The matrix solution was saturated in 40% CH_3CN, 0.1% trifluoroacetic acid (TFA) in water. The peptide solution (1.0 μL) was applied first to the smooth, sample plate target, then 1.0 μL of matrix solution was stirred in with a pipette tip and the sample was allowed to air-evaporate. MALDI experiments were performed on a PerSeptive Biosystems Voyager-DE STR time-of-flight mass spectrometer (2.0 m linear flight path) equipped with delayed ion extraction. A pulsed nitrogen laser (Model VSL-337ND; Laser Science, Franklin, MA) at 337.1 nm (<4 ns FWHM pulse width) was used for all of the data acquisition. Data were acquired in the delayed ion extraction mode using a 20 kV bias potential, a 6 kV pulse, and a 150 ns pulsed delay time. Dual microchannel plate (Model 3040MA; Burle Electro-Optics, Sturbridge, MA) detection was utilized in the reflector mode with the ion signal recorded using a 2 GHz transient digitizer (Model TDS 540C; Tektronix, Wilsonville, OR) at a rate of 1 GS/s. All mass spectra represent signal averaging of 128 laser pulses. The performance of the mass spectrometer produced sufficient mass resolution to produce the isotopic multiplet for each ion species below a mass-to-charge (*m/z*) of 3000. The data were analyzed using GRAMS/386 software (Galactic Industries, Salem, NH). All MALDI mass spectra were internally calibrated using masses from two trypsin autolysis products (monoisotopic masses 841.50 and 2210.10). Mass spectral peaks were determined based on a signal-to-noise ratio (S/N) of 3. Two software packages, Protein Prospector and Profound, were used to identify protein spots. The rat and mouse nonredundant (NR) database consisting of SWISS-PROT, PIR, GeneBank and OWL was used in the searches. Parameters used in the searches included proteins less than 100 kDa, greater than four matching peptides, and mass errors less than 45 ppm.

2.8 Sequence tagging using ESI-MS/MS

A home-built microelectrospray interface similar to an interface described by Gatlin *et al.* [16] was employed. Briefly, the interface utilizes a polyetheretherketone (PEEK) microtee (Upchurch Scientific, Oak Harbor, WA) into one stem of which is inserted a 0.025″ gold wire to supply the electrical connection. Spray voltage was 1.8 kV. A microcapillary column was prepared by packing 10 μm SelectPore particles (Vydac, Hesperia, CA) to a depth of 12 cm into a 75 × 360 μm fused silica capillary PicoTip (New Objectives, Cambridge, MA). The PicoTip has a 15 μm ID needle tip with an incorporated borosilicate glass frit. A 70 μL/min flow from a MAGIC 2002 HPLC solvent delivery system (Michrom BioResources, Auburn, CA) was reduced using a splitting tee to achieve a column flow rate of 450 nL/min. Samples were loaded on-column utilizing an Alcott model 718 autosampler (Alcott Chromatography, Norcross, GA). HPLC flow was split prior to sample loop injection. Samples prepared for MALDI were diluted 1:3 in 0.5% HOAc, and 2 μL of each sample was injected on-column. Using contact closures, the HPLC triggered the autosampler to make an injection and, after a set delay time, triggered the mass spectrometer to start data collection. A 12 min gradient of 5–55% solvent B (A: 2% ACN/0.5% HOAc; B: 90% ACN/0.5% HOAc) was selected for separation of trypsin-digested peptides. Peptide analyses were performed on a Finnigan LCQ ion trap mass spectrometer (Finnigan MAT, San Jose, CA). The heated desolvation capillary was set at 150°C, and the electron multiplier at –900 V. Spectra were acquired in automated MS/MS mode with a relative collision energy (RCE) preset to 35%. To maximize data acquisition efficiency, the additional parameters of dynamic exclusion, isotopic exclusion, and “top 3 ions” were incorporated into the auto-MS/MS procedure. For the “top 3 ions” parameter, an MS spectrum was taken, followed by three MS/MS spectra corresponding to the three most abundant ions above threshold in the full scan.

This cycle was repeated throughout the acquisition. The scan range for MS mode was set at *m/z* 375–1200. A parent ion default charge state of +2 was used to calculate the scan range for acquiring tandem MS. Automated analysis of peptide tandem mass spectra was performed using the SEQUEST computer algorithm (Finnigan MAT). The NR protein database was obtained as an ASCII text file in FASTA format from the National Center for Biotechnology Information (NCBI). A specific rat protein database was created by selecting rat protein sequences from the NR database. This database subset was used for subsequent searches. Protein identifications were based on obtaining a minimum of two unique tryptic peptides with SEQUEST scores greater than 3.0 from a protein present in the rat database.

3 Results and discussion

All animals tolerated and survived the treatment; however, a decrease in food consumption in the high dose group occurred, which led to a decrease in average weight gain in rats from this group. Over the 7-day treatment period the average weight gain was 28.8 g in control animals, 31.3 g in the low dose and 2.84 g in the high dose treatment group. Liver samples of all animals were analyzed individually. A schematic representation of a F344 rat liver 2-DE protein pattern is shown in Fig. 1, illustrating over 1000 Coomassie Blue-stained protein spots. Lovastatin treatment altered the abundance of 36 liver spots, based on the application of the two-tailed Student *t*-test (10 with $p<0.0001$ and 26 with $p<0.001$). All the

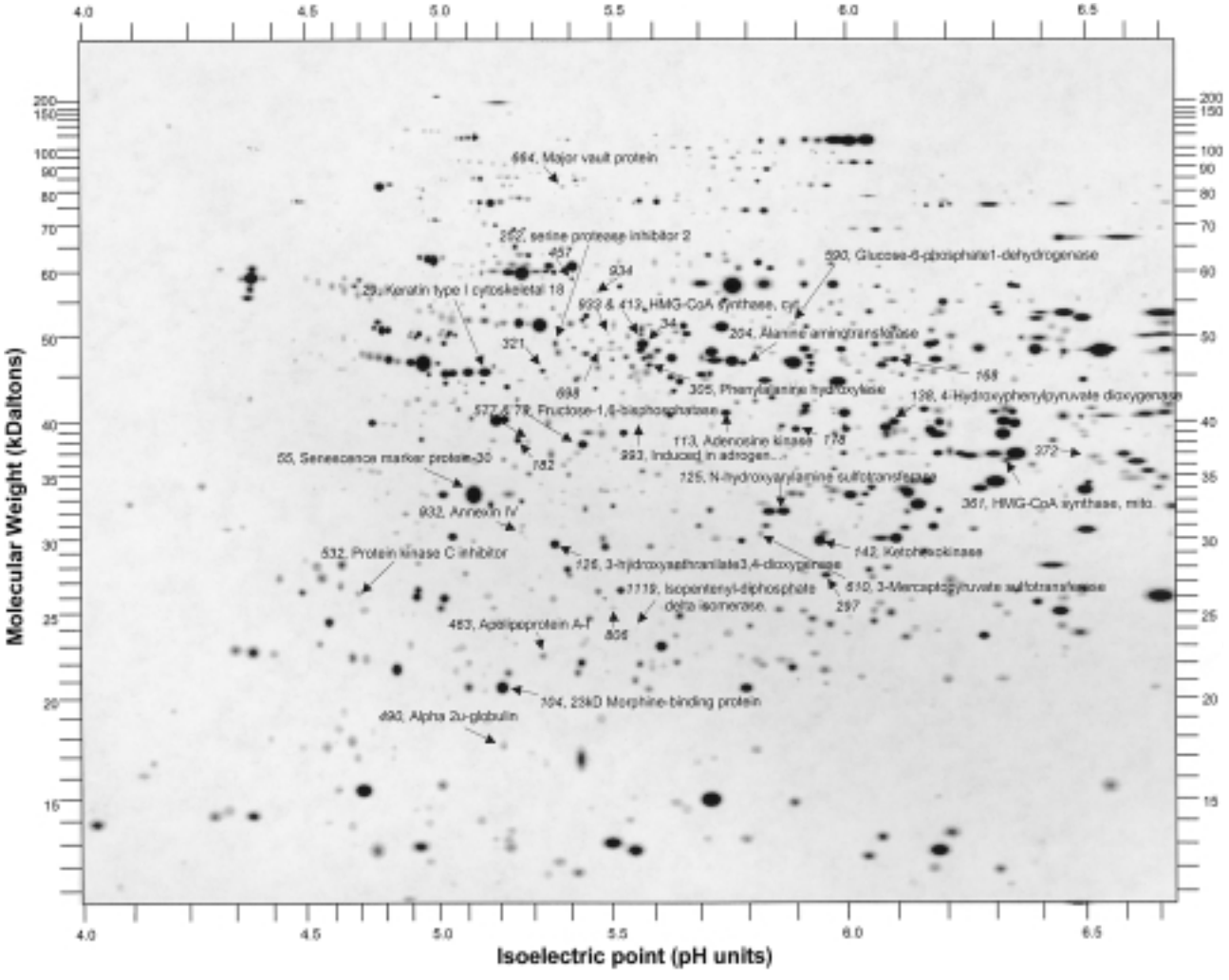

Figure 1. Schematic representation of the Coomassie-blue stained F344 rat liver reference pattern. Numbered and labeled protein spots were altered following treatment with lovastatin. Molecular mass and p*I* calibrations are estimated based on the calculated molecular mass and p*I* of a set of proteins identified in the pattern. Ratio and significance of the changed spots are listed in Table 1 and protein identifications are listed in Table 2.

statistically significant changes occurred in the group receiving 1500 ppm lovastatin in feed for seven days, an amount similar to the high dose used in the 24-month carcinogenicity study in rats [17]. Changes were evident in livers of rats treated with 16 ppm lovastatin for seven days, an exposure comparable to the maximum recommended daily dose in humans, but did not reach as high a level of statistical significance. The proteins affected by the treatment are indicated with spot numbers and protein names in Fig. 1 and are listed in Table 1. Several proteins have been previously identified in the F344 rat liver reference 2-D pattern [18]. Spots not yet identified but significantly affected by lovastatin treatment were subjected to tryptic digestion and MALDI-MS and ESI-MS/MS analysis. In this way more than half of the spots could be matched to known protein sequences and unambiguously identified (Table 2). Of the remaining spots some produced good peptides but did not match with rat sequences in public databases and some were too low in abundance to obtain useful data.

3.1 Cholesterol metabolism

Lovastatin treatment increased the abundance of both cytosolic and mitochondrial HMG-CoA synthase, two enzymes with similar functions but encoded by different genes [19]. HMG-CoA synthase drives the condensation of acetyl-CoA with acetoacetyl-CoA to form HMG-CoA, which is the substrate for HMG-CoA reductase. HMG-CoA reductase is a rate-limiting enzyme of the cholesterol synthesis pathway and converts HMG-CoA to mevalonate. While cytosolic HMG-CoA synthase is involved in the cholesterol biosynthesis pathway, mitochondrial HMG-CoA synthase is part of the ketone body synthesis pathway and was reported to be greatly increased by starvation, fat feeding and diabetes [20].

Isopentenyl-diphosphate delta-isomerase (IPP-isomerase), an enzyme participating in the cholesterol biosynthesis pathway downstream of HMG-CoA reductase and catalyzing the rearrangement of IPP to its allylic isomer, showed the most prominent treatment effect. In animals fed low doses of lovastatin its levels were induced around 2-fold and in the high dose group its increase was more than 20-fold. The strong induction of cytosolic HMG-CoA synthase and of IPP-isomerase following lovastatin treatment is likely a feedback reaction and an attempt of the liver to compensate for impaired cholesterol biosynthesis performance. The degree of the induction of these enzymes thus may reflect the HMG-CoA reductase inhibitor's pharmacological potency to inhibit HMG-CoA reductase and hence may serve as a marker to compare efficacy among different members of this family. It is likely that the inhibition of HMG-CoA reductase leads to a subsequent change in its protein abundance. HMG-CoA reductase is a transmembrane protein with a theoretical p*I* of 6.4; these two properties make it difficult to solubilize and focus well within the gel range used in this study. Changes in the current protocols may be necessary to visualize HMG-CoA reductase as well as other enzymes of the cholesterol synthesis pathway with a basic p*I*.

A protein related to cholesterol metabolism, apolipoprotein A–I, was found to be strongly induced by lovastatin. As most of the apolipoproteins, apolipoprotein A–I is synthesized in the liver and then secreted into the blood. Apolipoprotein A–I is the major protein of plasma HDL and is also found in chylomicrons. HDL mediates the reverse transport of cholesterol from tissues to the liver, the site where cholesterol is metabolized and secreted. Thus, the increased synthesis of precursor apolipoprotein A–I may suggest an upregulation of HDL synthesis and a subsequent increase in cholesterol catabolism in the liver. As discussed earlier, liver LDL receptors are expected to be upregulated following lovastatin treatment [1, 5]. The LDL receptor is a membrane protein that likely is not solubilized under the conditions used in this protocol and hence is missing in this data set. In addition to lovastatin, we have analyzed several members of the statin family (data not shown). All show a similar induction pattern of enzymes involved in cholesterol metabolism, although the degree to which individual enzymes were affected varies considerably.

3.2 Carbohydrate metabolism

Gene regulation effects induced by lovastatin were not restricted to the originally targeted cholesterol synthesis pathway but affected energy metabolism more globally. Treatment decreased fructose-1,6-bisphosphatase, a key regulatory enzyme of gluconeogenesis that catalyzes the hydrolysis of fructose-1,6-bisphosphate to generate fructose-6-phosphate and inorganic phosphate. Deficiency of fructose-1,6-bisphosphatase was found to be associated with fasting hypoglycemia and metabolic acidosis because of impaired gluconeogenesis [21]. A similar decrease was found in ketohexokinase an enzyme that catalyzes the phosphorylation of fructose to fructose-1-phosphate. On the other hand, glucose-6-phosphate 1-dehydrogenase, the first enzyme in the pentose phosphate pathway, was increased by lovastatin, suggesting the upregulation of the pentose phosphate pathway. The changes in carbohydrate metabolism seem at least in part related to the decrease in weight gain, emphasizing the importance of the confounding influence of food intake in the interpretation of the data.

Table 1. Changes in the rat liver proteome following treatment with lovastatin for 7 days

MSN[a)]	Protein name	Control		Lovastatin 1.6 mg/kg/day					Lovastatin 150 mg/kg/day				
		Avol.[b)]	CV[c)]	Avol.	CV	Prob.[d)]	Ratio[e)]	*N*-fold[f)]	Avol.	CV	Prob.	Ratio	*N*-fold
29	Keratin type I cytoskeletal 18	34239	0.141	32966	0.268	0.78	0.96	1.04	65975	0.099	0.00011	1.93	1.93
34		18202	0.159	17250	0.36	0.76026	0.95	1.06	7508	0.094	0.00015	0.41	2.42
55	Senescence marker protein-30	48659	0.089	55137	0.236	0.3232	1.13	1.13	28247	0.134	0.00016	0.58	1.72
79	Fructose-1,6-bisphosphatase (EC 3.1.3.11)	16910	0.048	15028	0.098	0.03478	0.89	1.13	8998	0.103	0.00002	0.53	1.88
104	23 kDa Morphine-binding protein	24001	0.074	26136	0.09	0.14285	1.09	1.09	31192	0.07	0.00071	1.3	1.3
113	Adenosine kinase (EC 2.7.1.20)	17090	0.047	13286	0.254	0.03824	0.78	1.29	11939	0.103	0.00016	0.7	1.43
125	*N*-hydroxyarylamine sulfotransferase (EC 2.8.2-)	23931	0.176	23395	0.139	0.82146	0.98	1.02	12205	0.155	0.00075	0.51	1.96
126	3-Hydroxyanthranilate 3,4-dioxygenase (EC 1.13.11.6)	10316	0.03	11324	0.127	0.1631	1.1	1.1	5729	0.259	0.00032	0.56	1.8
138	4-Hydroxyphenylpyruvate dioxygenase	10341	0.174	8922	0.316	0.62637	0.86	1.16	5870	0.079	0.00097	0.57	1.76
142	Ketohexokinase (EC 2.7.1.3)	18570	0.069	17063	0.297	0.542	0.92	1.09	10706	0.22	0.00037	0.58	1.73
168		12507	0.085	12603	0.233	0.94523	1.01	1.01	7802	0.082	0.00012	0.62	1.6
178		7939	0.069	7848	0.081	0.80706	0.99	1.01	4947	0.209	0.00072	0.62	1.6
182		6591	0.06	6817	0.094	0.52462	1.03	1.03	3311	0.216	0.0001	0.5	1.99
252	Serine protease inhibitor 2	4463	0.146	5415	0.175	0.09899	1.21	1.21	2356	0.074	0.00075	0.53	1.89
297		6936	0.048	6405	0.106	0.15292	0.92	1.08	4716	0.095	0.0001	0.68	1.47
305	Phenylalanine hydroxylase (EC 1.14.16.1)	16038	0.086	12967	0.237	0.07357	0.81	1.24	7513	0.098	0.00003	0.47	2.13
321		3083	0.049	3084	0.046	0.98549	1	1	4712	0.093	0.00017	1.53	1.53
361	HMG-CoA synthase, mitochondrial frag. (EC 4.1.3.5)	9198	0.4	7117	0.301	0.30701	0.77	1.29	25621	0.096	0.00032	2.79	2.79
372		13679	0.266	17782	0.409	0.29212	1.3	1.3	62468	0.06	0.0002	4.57	4.57
413	HMG-CoA synthase, cytosolic (EC 4.1.3.5)	5903	0.145	9113	0.539	0.18649	1.54	1.54	28598	0.089	0.00001	4.84	4.84
457		2618	0.05	2187	0.384	0.28826	0.84	1.2	3432	0.089	0.00089	1.31	1.31
463	Apolipoprotein A-I	3276	0.169	3125	0.152	0.65984	0.95	1.05	7826	0.162	0.00022	2.39	2.39
490	Alpha 2u-globulin	8370	0.284	10172	0.124	0.17027	1.22	1.22	1874	0.401	0.00065	0.22	4.47
532	Protein kinase C inhibitor	2344	0.142	2789	0.098	0.04797	1.19	1.19	4583	0.151	0.00038	1.96	1.96
577	Fructose-1,6-bisphosphatase (EC 3.1.3.11)	2191	0.16	2165	0.274	0.93334	0.99	1.01	935	0.415	0.00096	0.43	2.34
590	Glucose-6-phosphate 1-dehydrogenase (EC 1.1.1.49)	796	0.109	988	0.202	0.08237	1.24	1.24	2358	0.161	0.0001	2.96	2.96
610	3-Mercaptopyruvate sulfotransferase (EC 2.8.1.2)	2517	0.209	3008	0.101	0.14167	1.2	1.2	10242	0.103	0.00004	4.07	4.07
664	Major vault protein	1023	0.137	1049	0.258	0.84933	1.03	1.03	2008	0.095	0.00008	1.96	1.96
698		2059	0.094	2063	0.231	0.98501	1	1	5578	0.111	0.00003	2.71	2.71
806		913	0.146	748	0.362	0.26655	0.82	1.22	1710	0.15	0.00081	1.87	1.87
932	Annexin IV	716	0.179	1366	0.3	0.0278	1.91	1.91	2415	0.103	0.00014	3.37	3.37
933	HMG-CoA synthase, cytosolic (EC 4.1.3.5)	598	0.369	669	0.411	0.6649	1.12	1.12	3371	0.06	0.00001	5.64	5.64
934		461	0.438	880	0.273	0.02638	1.91	1.91	1164	0.125	0.0008	2.53	2.53
993	Induced in androgen-indep. prostate cells by eff. of apopt.	620	0.444	739	0.358	0.53959	1.19	1.19	1702	0.119	0.00026	2.74	2.74
1081		363	0.117	267	0.275	0.06977	0.74	1.36	757	0.208	0.00093	2.09	2.09
1119	Isopentenyl-diphosphate delta-isomerase (EC 5.3.3.2)	756	0.094	1709	0.372	0.10043	2.26	2.26	18052	0.106	0.00035	23.88	23.88

a) MSN, master spot number from F344MST3 liver
b) Group average of spot optical density value (arbitrary units)
c) coefficient of variation
d) *P*-value when compared to control (Student's *t*-test)
e) Ratio of change relative to control
f) Magnitude of change (the greater value of ratio or 1/(ratio of change))

3.3 Calcium homeostasis, apoptosis and cellular stress

Senescence marker protein-30 (SMP-30) is decreased in response to lovastatin treatment. SMP-30, a cytosolic protein with decreased expression during senescent stages, was recently reported to be identical to a calcium binding protein called regucalcin [22]. SMP30 is suggested to regulate calcium homeostasis by enhancing plasma membrane calcium-pumping activity [23]. Its downregulation in livers of rats treated with high doses of lovastatin could result in deregulation of calcium signaling and in cellular stress. The protein product of a gene with the name "induced in androgen-independent prostate cells by effectors of apoptosis" was induced in the liver of lovastatin treated animals. The induction of this gene has been shown to be apoptosis-specific [24], suggesting that high doses of lovastatin trigger apoptosis in liver cells of treated rats. Similar observations have been reported from *in vitro* experiments with lovastatin [25]. As elevation of intracellular calcium is central to apoptosis, this event is likely the consequence of the treatment-related disturbance of calcium homeostasis as reflected by the decrease in SMP-30 levels. Serine protease inhibitors (serpins) are a family of proteins that function to control the action of serine proteases in many diverse physiological processes. The expression of serine protease inhibitor 2 (SPI-2) was reported to be downregulated in inflammation. The treatment-related decrease in SPI-2 may indicate that high doses of lovastatin induce inflammatory processes in liver. However, histopathological examinations of liver slices would be necessary to confirm this.

3.4 Cytoskeletal structure and membrane trafficking

Keratin type I cytoskeletal 18 and of major vault protein abundances were increased upon treatment with high doses of lovastatin. Cytokeratin 18 is a subunit of cytokeratin filaments which are important components of the cytoskeletal structure. Major vault protein is required for normal vault structures, large ribonucleoprotein particles that may be involved in nucleocytoplasmic transport. The treatment-mediated changes of these proteins may reflect cellular stress induced with high doses of lovastatin. Lovastatin treatment was associated with a dose-dependent increase in annexin IV. The annexins are a group of homologous proteins that bind membranes and aggregate vesicles in a calcium-dependent fashion and contain a binding site for calcium and phospholipid. Annexins provide a major pathway for communication between cellular membranes and their cytoplasmic environment and are implicated in membrane-related events along exocytotic and endocytotic pathways. The induction of annexin IV may be related to the anticipated upregulation of the LDL receptor and a subsequent increase in endocytosis-mediated transport of cholesterol-carrying lipoprotein into liver cells.

3.5 Nucleotide and amino acid metabolism

Adenosine is an endogenous modulator of intercellular signaling that provides homeostatic reductions in cell excitability during tissue stress and trauma. The inhibitory actions of adenosine are mediated by interactions with

Table 2. MALDI-MS and ESI-MS data obtained from rat liver protein spots changed by lovastatin

MSN[a]	Protein name	Accession #[b]	Mol. mass[c] (Da)	p*I*[d]	MALDI[e]		ESI[f]	
					# M. pep.[g]	% S. C.[h]	# M. pep.	% S. C.
138	4-Hydroxyphenylpyruvate dioxygenase	gi 3435296	45 112	6.29			3	11
252	Serine protease inhibitor 2	sp P05545	43 773	5.39	12	40	7	24
305	Phenylalanine hydroxylase (EC 1.14.16.1)	sp P04176	51 821	5.76	15	42	12	26
361	HMG-CoA synthase, mitochondrial frag. (EC 4.1.3.5)	sp P22791	52 714	8.24			4	8
463	Apolipoprotein A-I	sp P04639	27 394	5.51	14	43	6	20
490	Alpha 2u-globulin	sp P02761	18 730	5.48			6	40
532	Protein kinase C inhibitor	sp P35214	28 171	4.8			2	4
577	Fructose-1,6-bisphosphatase (EC 3.1.3.11)	sp P19112	39 478	5.54			5	10
590	Glucose-6-phosphate 1-dehydrogenase (EC 1.1.1.49)	sp P05370	59 244	5.97			7	16
610	3-Mercaptopyruvate sulfotransferase	sp P97532	32 809	5.88			5	17
664	Major vault protein	sp Q62667	98 504	5.65			11	18
932	Annexin IV	sp P55260	35 743	5.32	7	41	6	23
993	Induced in androgen-indep. prostate cells by eff. of apopt.	gi 456282	35 866	5.6			3	12
1119	Isopentenyl-diphosphate delta-isomerase (EC 5.3.3.2)	sp O35760	26 402	5.57	6	14	6	20

a) MSN, master spot number
b) sp, SWISS-PROT; gi, GeneBank
c) Theoretical molecular mass
d) Theoretical p*I*
e) Identification by MALDI-MS
f) Identification by ESI-MS/MS
g) Number of peptides matching
h) % Sequence coverage

specific cell-surface G-protein coupled receptors regulating membrane cation flux, polarization, and the release of excitatory neurotransmitters. Adenosine kinase is the key intracellular enzyme regulating intra- and extracellular adenosine concentrations. Inhibition of adenosine kinase produces marked increases in extracellular adenosine levels that are localized to cells and tissues and undergoing accelerated adenosin release [26]. Thus it may be speculated that the downregulation of adenosine kinase following treatment with lovastatin could be an attempt of the liver to selectively enhance the protective actions of adenosine during stress. 3-Hydroxyanthranilate 3,4-dioxygenase, an enzyme of tryptophan metabolism that catalyzes the synthesis of excitotoxin quinolinic acid (QUIN) from 3-hydroxyanthranilic acid, is decreased in livers of lovastatin treated rats. A similar decrease is found in phenylalanine hydroxylase, a key enzyme in phenylalanine metabolism. It remains unclear why lovastatin treatment is downregulating these two enzymes in liver and what implications this effect may have.

3.6 Cell signaling

Lovastatin increased the levels of protein kinase C inhibitor, a protein that acts as a regulator of the cell signaling process. Protein kinase C inhibitor activates tyrosine and tryptophan hydroxylases in the presence of calcium/calmodulin-dependent protein kinase II, and strongly activates protein kinase C. The 23 kDa morphine binding protein, a member of the phosphatidylethanolamine-binding protein (PEBP) family is increased upon treatment with lovastatin. A variety of biological roles have been described for members of this family, including lipid binding, membrane signal transduction, roles as odorant effector molecules or opioids and interaction with the cell-signaling machinery [27]. The alterations in these proteins indicate that lovastatin affects cell signaling.

3.7 Biotransformation

N-hydroxyarylamine sulfotransferase, a liver specific enzyme involved in the biotransformation of endogenous and foreign substrates, is decreased and 3-mercaptopyruvate sulfotransferase, an enzyme involved in thiosulfate synthesis, is strongly increased by high doses of lovastatin. The relevance of this observation is unclear at this point. Alpha-2u globulin is synthesized in the liver of male but not female rats, secreted into the bloodstream and excreted in the urine [28]. It binds pheromones that are released from drying urine and affect the sexual behavior of females. There are a number of chemicals that induce a toxic syndrome in male rats referred to as α_{2u}-globulin nephropathy. This organ-specific toxicity is characterized by an accumulation of protein droplets in the proximal tubules. It was suggested that these droplets might be formed by the association between the chemical and the α_{2u} protein [29]. High doses of lovastatin strongly decrease the abundance of alpha-2u globulin in liver suggesting a down regulation of its synthesis or its increased secretion for yet unknown reasons.

4 Concluding remarks

Proteome analysis revealed quantitative alterations in a high number of hepatic proteins following treatment of rats with the lipid lowering agent and marketed pharmaceutical lovastatin (Mevacor®) for 7 days. The protein spots affected by the treatment were identified and grouped based on cellular function and participation in biochemical and signaling pathways. Of great interest was the observation that the inhibition of the enzyme HMG-CoA by lovastatin provoked a regulatory response in the cholesterol synthesis pathway including the strong induction of the enzymes cytosolic HMG-CoA synthase and IPP-isomerase. The fact that one of each enzyme is located downstream or upstream of the blockade demonstrates the rigorous attempt of the liver to maintain normal cholesterol synthesis rates. This new insight into cholesterol pathway regulation suggests that HMG-CoA synthase and IPP-isomerase may be alternative drug targets to be explored in order to control cholesterol synthesis. In fact, reports are available documenting that HMG-CoA synthase has been evaluated as a target for therapeutic intervention [30]. Attempts to therapeutically target IPP-isomerase have, to our knowledge, not been reported in the public domain. The effect of IPP-isomerase inhibition on the overall cholesterol synthesis rate is not clear at this point but the current data encourage further investigation of such a scenario. The response of the liver to lovastatin treatment was not restricted to the therapeutically targeted pathway but was extended to key enzymes regulating energy metabolism such as fructose-1,6-bisphosphatase, glucose-6-phosphate 1-dehydrogenase, and ketohexokinase. It is not surprising that manipulations of the lipid metabolism, a key player in energy homeostasis, equally affect related pathways such as carbohydrate metabolism, although the influence of reduced food consumption in treated animals may at least in part contribute to this effect. As with many pharmaceuticals, high doses of lovastatin were associated with early signs of toxicity as reflected by changes in a heterogeneous set of cellular stress proteins involved in functions such as cytoskeletal structure, calcium homeostasis, protease inhibition, cell signaling, and apoptosis. These data present new insights into liver gene network regulations induced by lovastatin and illustrate a yet unexplored use of proteomics to discover new targets by analysis of existing drugs and the pathways that they regulate.

Received January 10, 2000

5 References

[1] Goldstein, J. L., Brown, M. S., *J. Lipid Res.* 1984, *25*, 1450–1461.

[2] Sirtori, C. R., *Pharmacol. Res.* 1990, *22*, 555–563.

[3] Slater, E. E., MacDonald, J. S., *Drugs* 1988, *36*, 72–82.

[4] Swislocki, A. L., Lin, K., Cogburn, D., Fann, K. Y., Khuu, D. T., Noth, R. H., *Am. J. Manag. Care* 1997, *3*, 1537–1545.

[5] Goldstein, J. L., Brown, M. S., *Nature* 1990, *343*, 425–430.

[6] Arce, A., Aicher, L., Wahl, D., Anderson, N. L., Mehens, L., Raymackers, J., Cordier, A., Steiner, S., *Life Sci.* 1998, *63*, 2243–2250.

[7] Anderson, N. L., Taylor, J., Hofmann, J. P., Esquer-Blasco, R., Swift, S.,. Anderson, N. G., *Toxicol. Pathol.* 1996, *24*, 72–76.

[8] Anderson, N. L., Esquer-Blasco, R., Richardson, F., Foxworthy, P., Eacho, P., *Toxicol. Appl. Pharmacol.* 1996, *137*, 75–89.

[9] Steiner, S., Wahl, D., Mangold, B. L., Robison, R., Raymackers, J., Meheus, L., Anderson, N. L., Cordier, A., *Biochem. Biophys. Res. Commun.* 1996, *218*, 777–782.

[10] Aicher, L., Wahl, D., Arce, A., Grenet, O., Steiner, S., *Electrophoresis* 1998, *19*, 1998–2003.

[11] Myers, T. G., Dietz, E. C., Anderson, N. L., Khairallah, E. A., Cohen, S. D., Nelson, S. D., *Chem. Res. Toxicol.* 1995, *8*, 403–413.

[12] Cunningham, M. L., Pippin, L. L., Anderson, N. L., Wenk, M. L., *Toxicol. Appl. Pharmacol.* 1995, *131*, 216–223.

[13] Anderson, N. L., Esquer-Blasco, R., Hofmann, J. P., Anderson, N. G., *Electrophoresis* 1991, *12*, 907–930.

[14] Shevchenko, A., Wilm, M., Vorm, O., Mann, M., *Anal. Chem.* 1996, *68*, 850–858.

[15] Karas, M., Hillenkamp, F., *Anal. Chem.* 1988, *60*, 2299–2301.

[16] Gatlin, C. L., Kleemann, G. R., Hays, L. G., Link, A. J., Yates III, J. R., *Anal. Biochem.* 1998, *263*, 93–101.

[17] *Physicians' Desk Reference*, Edition 54, Medical Economics, Montvale, NJ 2000, p. 1836.

[18] Anderson, N. L., Esquer-Blasco, R., Hofmann, J. P., Meheus, L., Raymackers, J., Steiner, S., Witzmann, F., Anderson, N. G., *Electrophoresis* 1995, *16*, 1977–1981.

[19] Ayte, J., Gil-Gomez, G., Haro, D., Marrero, P. F., Hegardt, F. G., *Proc. Natl. Acad. Sci. USA* 1990, *87*, 3874–3878.

[20] Casals, N., Roca, N., Guerrero, M., Gil-Gomez, G., Ayte, J., Ciudad, C. J., Hegardt, F. G., *Biochem. J.* 1992, *283*, 261–264.

[21] el-Maghrabi, M. R., Lange, A. J., Jiang, W., Yamagata, K., Stoffel, M., Takeda, J., Fernald, A. A., Le Beau, M. M., Bell, G. I., Baker, L., *et al., Genomics* 1995, *27*, 520–525.

[22] Fujita, T., Shirasawa, T., Maruyama, N., *Mech. Aging Dev.* 1999, *10*, 7271–7280.

[23] Fujita, T., Inoue, H., Kitamuar, T., Sato, N., Shimosawa, T., Maruyama, N., *Biochem. Biophys. Res. Commun.* 1998, *250*, 374–380.

[24] Sells, S. F., Wood Jr. D. P., Joshi-Barve, S. S., Muthukumar, S., Jacob, R. J., Crist, S. A., Humphreys, S., Rangnekar, V. M., *Cell Growth Differ.* 1994, *5*, 457–466.

[25] Wang, W., Macaulay, R. J., *Can. J. Neurol. Sci.* 1999, *26*, 305–310.

[26] Kowaluk, E. A., Bhagwat, S. S., Jarvis, M. F., *Curr. Pharm. Des.* 1998, *4*, 403–416.

[27] Banfield, M. J., Barker, J. J., Perry, A. C., Brady, R. L., *Structure* 1998, *6*, 1245–1254.

[28] Roy, A. K., Neuhaus, O. W., *Proc. Soc. Exp. Biol. Med.* 1966, *121*, 894–899.

[29] Borghoff, S. J., Short, B. G., Swenberg, J. A., *Annu. Rev. Pharmacol. Toxicol.* 1990, *30*, 349–367.

[30] Greenspan, M. D., Yudkovitz, J. B., Lo, C. Y., Chen, J. S., Alberts, A. W., Hunt, V. M., Chang, M. N., Yang, S. S., Thompson, K. L., Chiang, Y. C., *et al., Proc. Natl. Acad. Sci. USA* 1987, *84*, 7488–7492.